

Potential activity of a selected natural compounds on SARS-CoV-2 RNA-dependent-RNA polymerase, and binding affinity of the receptor-binding domain (RBD)

Hisham Altayeb (✉ hdemmahom@kau.edu.sa)

King Abdulaziz university

Lamjed Bouslama

Laboratory of Bioactive Substances, Center of Biotechnology of Borj Cedria, University of Tunis El Manar, Tunisia

Jawaher Abdulbaqi Abdulhakim

Medical Laboratory Department, College of Applied Medical Sciences, Yanbu, Taibah University, Medina, KSA

Kamel Chaieb

Department of Biochemistry, Faculty of Science, King Abdulaziz University, Building A 90, Jeddah 21589, Saudi Arabia

Othman A. S. Baothman

Department of Biochemistry, Faculty of Science, King Abdulaziz University, Building A 90, Jeddah 21589, Saudi Arabia

Mazin A. Zamzami

Department of Biochemistry, Faculty of Science, King Abdulaziz University, Building A 90, Jeddah 21589, Saudi Arabia

Research Article

Keywords: Coronavirus, SARS-COV2, In silico, Molecular Docking, Natural compounds, Antiviral

Posted Date: June 4th, 2020

DOI: <https://doi.org/10.21203/rs.3.rs-32971/v1>

License: © ⓘ This work is licensed under a Creative Commons Attribution 4.0 International License. [Read Full License](#)

Abstract

Coronavirus disease (COVID-19) is caused by SARS-CoV-2 and represents the causative agent of a potentially lethal disease. COVID-19 has been described as a significant global public health pandemic by the World Health Organization due to its high mortality rate, rapid spread, and the lack of drugs and vaccines for it. Active antiviral drugs are desperately needed to combat the potential return of severe acute respiratory syndrome (SARS).

In this study, we selected 39 natural compounds present in plants, algae, and sponges with antiviral activity. Molecular docking was used to screen the compounds' activity on SARS-CoV-2 RNA-dependent-RNA polymerase, receptor-binding domain (RBD), and the human ACE2 receptor. Compounds with binding energy ≤ -6.5 kcal/mol enter pre-clinical testing using *in silico* ADME/Tox (absorption, distribution, metabolism, excretion, and toxicity).

We found eight potential SARS-CoV-2 inhibitors: (glycyrrhizin, rutin, baicalin, 1, 6-di-O-galloyl-beta-D-glucose, pyrophephorbide A, pheophorbide A, beta-Sitosterol, and vitexin). These outcomes indicate that these compounds could be potential candidates to be utilized in lead optimization for the design and production of the anti-SARS-CoV-2 drug.

1. Introduction

In December 2019, a new coronavirus (2019-nCoV) infection was reported in hospitalized patients with pneumonia of unknown cause in Wuhan, Hubei Province, China ¹. On January 30, 2020, the World Health Organization (WHO) officially declared the COVID-19 epidemic a global health emergency ².

COVID-19 is the name given to this novel coronavirus (CoV), spread throughout the world. Coronaviruses are enveloped RNA that belongs to the subfamily *Coronavirinae* of the family *Coronaviridae*; they broadly commonly spread by humans, birds, and other mammals, causing respiratory and intestinal infections in both animals and humans ³. Six species of coronavirus are known to cause human disease ⁴. Two of them are highly pathogenic and have previously caused extreme acute respiratory syndrome coronavirus (SARS-CoV) in 2002 and 2003 in Guangdong Province, China ^{5,6}, and Middle East respiratory syndrome coronavirus (MERS-CoV) in the Middle East in 2012 ⁷. These two viruses have been linked in some cases to fatal illness (Cui et al., 2019). The other four species (HCoV-229E, HCoV-OC43, HCoV-NL63, and HCoV-HKU1) are prevalent and typically induce only mild upper respiratory diseases in immunocompetent hosts ⁴.

COVID-19 is a β -coronavirus (CoV) that causes self-limiting upper infections in immunocompetent hosts. Severe symptoms such as breathing difficulty and pneumonia occur in immunocompromised and elderly persons and those with chronic underlying diseases. Moreover, the touching of contaminated objects seems to characterize the propagation of COVID-19 ⁸.

The angiotensin-converting enzyme 2 (ACE2) is an enzyme that transforms angiotensin II into angiotensin (1-7) ^{9,10}. Angiotensins are peptides involved in maintaining blood pressure control and arterial hypertension by increasing the secretion of aldosterone ¹¹ and promoting sodium retention by the kidneys ¹². ACE2 receptors are attached to the surfaces of the lungs, heart, and kidney cell membranes ^{13,14}.

The spike (S) glycoprotein of SARS-CoV-2 contains the receptor-binding domain (RBD) that recognize specific cell receptors for its attachment. Angiotensin is peptides involved in membrane fusion and entry process through endocytosis ¹⁵. It has been reported that ACE2 is the receptor of the SARS-CoV-2 S glycoprotein ^{16,17} due to the presence of affinity domains ¹⁸.

The interaction of this spike protein with ACE2 could be responsible for lung damage ¹⁹. Therefore, the RBD of spike glycoprotein could be a candidate for drug targets for inhibiting the initiation process of virus infection ²⁰.

In the absence of antiviral treatment, infected patients receive oxygen therapy and immunoglobulin G for critical cases ²¹. Antiviral drugs were previously tested in clinical practice, including nucleoside analogs acting as polymerase inhibitors, such as ribavirin (hepatitis C virus), acyclovir (herpes virus), ganciclovir (cytomegalovirus), and favipiravir (Ebola and influenza A virus); protease inhibitors, such as lopinavir and ritonavir (human immunodeficiency virus, SARS, and MERS), and nafamostat (influenza virus and Ebola); and neuraminidase inhibitors, such as oseltamivir (influenza virus A). However, all of the tests using these molecules were invalid for COVID-19. By contrast, the best results were obtained with the non-antiviral drug chloroquine, which has been used since the 1950s to treat malaria ²². Nevertheless, its antiviral mechanism is not well understood; however, we suppose that this compound inhibits pH-dependent steps of the virus replication ²³ or interferes with the glycosylation of cellular receptors ²⁴. *In vitro* studies also demonstrated that chloroquine acts at both entry and post-entry stages of the COVID-19 infection on Vero cells ²⁵. Remdesivir, which is an adenosine nucleotide analog prodrug, has been reported to exhibit activity against several RNA viruses ²⁶ by inhibiting RNA polymerase activity ²⁷.

This study aimed to *in silico* evaluate the effect of 39 natural compounds, which have been reported to exhibiting *in vitro* antiviral activity, on the SARS-CoV-2 RNA-dependent-RNA polymerase activity as well as on their interaction with RBD and ACE2. The compounds, which displayed a binding energy more than 6.5 Å, were tested for absorption, plasma clearance, tissue distribution, metabolic effects, toxicity, and drug-likeness using [Pre ADMET](#) profiling.

2. Materials And Methods

2.1. Natural products and active molecules with antiviral activity

Thirty-nine natural compounds isolated from plants, algae, and sponges (Table 1) and three antiviral drugs (Velpatasvir, IDX-184, and Oseltamivir) have been tested by *in silico* for their inhibitory activity on SARS-CoV-2 RNA-dependent-RNA polymerase activity, as well as RBD and ACE2 interaction.

Table1: Selected natural products displayed antiviral activities

Origin	Natural compound	Targeted Virus	References	
<i>Acacia nilotica</i> (Plant)	6-di-O-galloyl-beta-D-glucose	-Anti Hepatitis C virus (HCV), Anti HIV-1	28,29	
	Melacacidin			
	Digallic acid			
	Ellagic acid			
	Ethyl gallate			
	Gallic acid			
<i>Nigella sativa</i> (Plant)	Beta-Sitosterol	AIV (H9N2)	30	
	Dithymoquinone			
	Thymohydroquinone			
	Thymol			
<i>Commiphora gileadensis</i> (Plant)	Guggulsterone E	HSV-2	31	
		RSV-B		
<i>Opuntia ficus indica</i> (Plant)	Pheophorbide A	HSV-2	31	
	Pyropheophorbide A	IIFV-A		
<i>Salvadora persica</i> L., (Plant)	Benzylisothiocyanate	HSV-1	32	
<i>Peganum harmala</i> (Plant)	Harmine	HSV-2	33	
<i>Lycoris radiata</i> (Plant)	Lycorine	SARS-CoV	34	
	Glycyrrhizin			
<i>Eugenia caryophyllus</i> (Plant)	Eugenol	HSV	35	
<i>Flos Lonicerae</i> (Plant)	Chlorogenic acid	SARS-CoV	36	
<i>Punica granatum</i> (Plant)		Punicalagin	HEV-71	37
<i>Scutellaria baicalensis</i> (Plant)		Baicalin	SARS-CoV	36
<i>Brassica oleracea</i> (Plant)		Sulforaphane	IFV-A	38
<i>Cladosiphon okamuranus</i> (Brown algae)		Fucoidan	NDV	39
<i>Pseudodistoma antinboja</i> (Sponge)		Butenolides	IFV-A (H1N1)	40
Honey (Bee product)		Rutin	VZV	41,42
		Acacetin	IFV	
		Apigenin		
		Catechin		
		Chrysin		
		Hispidulin		
		Kaempferol		
		Luteolin		
		Myricetin		
		Naringetol		
		Quercetin		
	Tricetin			
	Vitexin			

AIV: Avian influenza virus; HCV: hepatitis C virus; HSV: herpes simplex virus; HEV: human enterovirus; IFV: influenza virus; NDV: Newcastle disease virus; RSV: respiratory syncytial virus; VZV: varicella-zoster virus

2.1 Homology modeling

The structures of SARS-CoV-2 RNA-dependent RNA polymerase (RdRp) (7BV2), spike protein model (6VSB) and human ACE2 receptor (6VW1) in complex with RBD of SARS-CoV-2, were obtained from the [RCSB PDB database](#) ⁴³.

2.2 Preparation of proteins and inhibitors

The structures of RdRp, ACE2, and the SARS-CoV-2 spike protein were prepared for docking by protonation, water molecules removal, atom fixation, RMSD gradients refinement, and energy minimization by the drug discovery platform Molecular Operating Environment (MOE) suite (demo version 2019; Chemical Computing Group Inc: Montreal, QC, Canada). Thirty-nine natural products compounds (Table 1) and three antiviral references (Velpatasvir, IDX-184, and Oseltamivir) structures were obtained from the [PubChem database](#) ⁴⁴.

2.3 Molecular docking

The default docking parameters in MOE were used to study the best stable conformational binding (poses with the lowest energy level) between ligands and protein receptors. Docking with root-mean-square deviation (RMSD) less than 2 Å, was considered a success ⁴⁵. Known and predicted active sites and interacting residues were used for ligand docking ¹⁷.

2.4 Protein-Ligand interaction analysis

The binding affinities, visualization, and interactions of ligand-receptor complexes were examined by the [Protein-Ligand Interaction Profiler \(PLIP\)](#) web server (Salentin et al., 2015), and Discovery Studio Visualizer 2020 ([BIOVIA, 2017](#)). Compounds with the most favorable binding energy (≤ -6.5 kcal/mol), were selected for further analysis ⁴⁶.

2.5 ADMET Profiling

To assess the potential pharmacokinetic properties of the top eight compounds (that scored the lowest energy ≤ -6.5), we conducted a preliminary computational screening using [PreADMET](#) profiling to estimate their absorption rate, plasma clearance, tissue distribution, metabolic effects, toxicity, and drug likeness ⁴⁷⁻⁴⁹.

3. Results And Discussion

3.1.1 Target proteins active site prediction

MOE software site finder specified the following residues in the active site of the SARS-CoV-2 RdRp: ASP161, TYR163, ASP164, PHE165, GLU167, LYS551, ARG553, GLY616, TRP617, ASP618, TYR619, PRO620, LYS621, ASP760, ASP761, ALA762, VAL763, VAL792, PHE793, MET794, SER795, ALA797, LYS798, CYS799, TRP800, HIS810, GLU811, and PHE812. The active sites of SARS-CoV-2 spike protein RBD and ACE2 receptor were determined according to previously published data ^{43,50}.

3.1 Docking and interaction analysis

From 39 natural compounds virtually screened for their activities on RdRp, ACE2, and RBD proteins, only eight hits scored binding energy ≤ -6.5 kcal/mol (Table 2). Then the promoting eight compounds were selected for further interaction analysis and PreADMET profiling.

Table 2: Molecular Docking results and PubChem ID of the selected compounds and some antiviral agents

No	Compounds	RdRp		ACE2		RBD-SARS-CoV-2		
		PubChem ID	S	RMS D	S	RMS D	S	RMS D
1	Glycyrrhizin	14982	-7.9	2.0	-7.8	1.8	-7.3	2.3
2	Rutin	5280805	-7.8	2.0	-6.9	2.9	-6.9	1.5
3	Baicalin	64982	-7.6	1.3	-6	2.4	-6.4	1.0
4	1,6-di-O-galloyl-beta-D-glucose	440221	-7.5	2.9	-6.3	1.7	-6.2	1.7
5	Pheophorbide A	253193	-7.3	1.0	-6.5	3.5	-6.6	2.0
6	Pyropheophorbide A	161456	-7.3	1.4	-6.2	2.0	-6.4	1.5
7	Beta-Sitosterol	222284	-6.9	1.5	-6	3.9	-5.9	1.8
8	Vitexin	5280441	-6.5	2.4	-5.6	1.5	-5.6	2.7

9	Chlorogenic acid	1794427	-6.4	1.5	-5.7	1.8	-5.9	1.9
10	Dithymoquinone	398941	-6.2	1.4	-4.7	2.4	-5.2	0.9
11	Hispidulin	5281628	-6	1.1	-5.2	1.5	-5.4	3.1
12	Melacacidin	169996	-5.8	1.3	-5	2.5	-5.1	1.5
13	Catechin	9064	-5.8	2.4	-5.1	1.4	-5.1	1.9
14	Fucoidan	92023653	-5.8	1.5	-5.2	1.8	-5.1	4.9
15	Gallic acid	370	-5.5	0.6	-4	4.4	-4.2	2.4
16	Methyl gallate	7428	-5.7	1.6	-5.4	1.7	-4.8	2.4
17	Trans,Trans-Farnesol	445070	-5.7	1.3	-5.3	1.3	-5.4	1.6
18	Digallic acid	341	-5.6	1.1	-5.5	1.2	-5.3	2.5
19	Myricetin	5281672	-5.6	2.7	-5.2	1.7	-5.2	1.6
20	Ellagic acid	5281855	-5.5	0.6	-4.8	0.8	-4.9	1.8
21	Ethyl gallate	13250	-5.3	1.3	-4.2	1.0	-4.7	1.4
22	Thymoquinone	10281	-5.0	1.3	-4.4	1.0	-4.4	0.6
23	Acacetin	5280442	-5.4	2.8	-5.0	1.3	-5.2	1.9
24	Apigenin	5280443	-5.4	1	-5.0	2.5	-4.9	1.4
25	Chrysin	5281607	-5.1	1.6	-4.8	1.6	-4.9	1.2
26	Kaempferol	5280863	-5.4	2.5	-5.2	1.4	-5.2	0.9
27	Luteolin	5280445	-5.3	2.4	-5.2	1.1	-5.0	1.4
28	Naringetol	439246	-5.7	1.5	-5.1	0.9	-5.1	1.1
29	Quercetin	5280343	-5.6	1.2	-5.0	2.4	-5.4	1.2
30	Tricetin	5281701	-5.3	2.0	-5.2	0.6	-5.2	1.1
31	Guggulsterone E	6439929	-5.5	2.0	-4.9	1.2	-5.2	3.1
32	Benzylisothiocyanate	2346	-5.2	3.9	-4.2	1.2	-4.4	1.6
33	harmine	5280953	-5.5	2.4	-4.5	2.1	-4.7	1.0
34	lycorine	72378	-5.4	4.9	-4.8	2.3	-5.2	1.5
35	Eugenol	3314	-5.4	1.0	-4.2	1.1	-4.5	0.9
36	Butenolides	386024422	-5.6	1.4	-4.5	0.9	-4.5	1.3
37	Sulforaphane	5350	-5.3	2.3	-4.4	1.6	-4.7	1.2
38	Thymol	6989	-4.5	1.0	-4.1	3.9	-4.5	1.5
39	Thymohydroquinone	95779	-4.8	2.9	-4.4	1.2	-4.4	1.9
Antiviral agents								
40	Velpatasvir	67683363	-9.3	1.7	-	-	-5.5	2.0
41	IDX-184	135565589	-8.8	2.5	-	-	-6.6	4.0
42	Oseltamivir	65028	-6.5	2.1	-	-	-5.1	2.2

Abbreviations: *S*= binding score in kcal/mol, *RdRp*= RNA-dependent-RNA polymerase, *RBD*= Receptor binding Domain of virus spike protein

3.3 Interactions of ligands and RNA-dependent RNA polymerase (RdRp)

As shown in Table 3, the docking results of glycyrrhizin show the lowest binding affinity (-7.9) among all of the screened compounds that forming many hydrogen bonds, alkyl, and carbon hydrogen bond (Figure 1). Docking of glycyrrhizin is considered successful with RMSD 2 (dockings with RMSDs 2Å are considered a successful, docking with RMSD 2-3Å are considered a partial success)⁵¹. The activity of glycyrrhizin on SARS-CoV-2 polymerase, aligned with previous studies, confirmed the activity of glycyrrhizin on the replication of SARS-CoV and polymerase of influenza virus^{52,53}. Rutin with RdRp active site showed the second-lowest binding energy, at -7.8; this was a result of the formation of two conventional hydrogen bonds, two pi-alkyl, one pi-donor hydrogen bond, three pi-cation bonds, and five carbon-hydrogen bonds with residues located at the conserved pocket of RdRp⁵⁴. The docking of rutin is considered successful with RMSD 2 Å (Table 3) (Figure 2).

Baicalin formed a strong interaction with protein active site, which scored low binding energy (-7.6) and RMSD 1.3. Baicalin strong interaction and well configuration in protein pocket occurred due to the presence of six hydrogen bonds with distances less than 3.33 Å. In addition to the presence of H bonds, there were many other types of bonds, such as pi-alkyl, pi-sigma, Pi-cation, pi-anion, pi-pi t-shaped, pi-lone pair, carbon hydrogen bond (Table 3) (Figure 3).

Table 3. Interaction of active compounds with SARS-CoV-2 RdRp.

Compounds (PubChem ID)	S	RM SD	Protein ligands interaction		Distance (Å)
			Type of interaction	Amino acid residues (No. of bonds)	
Glycyrrhizin (14982)	-7.9	2.1	Conventional hydrogen bonds	TYR619 (1), LYS621 (1), ASP684 (1), ALA688 (1), ARG624, ARG553(1) ASP760 (2)	3.03, 2.61, 2.95, 2.42, 2.97, 2.41 2.75, 2.10
			Alkyl	ARG555, ALA688	3.49, 4.95
			Carbon Hydrogen bonds	THR687(1), ASP623 (3), ARG533(1)	2.47, 2.65, 2.22, 2.25, 2.53,
Rutin (5280805)	-7.8	2.0	Conventional hydrogen bonds	TYR619(1), ARG553(1)	2.27, 2.16
			Pi-Alkyl	LYS621 (1), ARG553	4.47, 4.2
			Pi-Donor Hydrogen bond	PRO620 (1)	2.82
			Pi-Cation	LYS621(1), ARG553 (2)	4.52, 3.89
			Carbon Hydrogen bond	ASP760 (2), ASP623(1), LYS621 (2)	2.51, 2.66, 2.60, 2.91, 2.80
Baicalin (64982)	-7.6	1.3	Conventional hydrogen bonds	TYR455 (1), ALA554 (1) ARG553 (2) ARG624 (2)	3.33, 1.99 2.44, 2.85 2.33, 2.26, 3.72
			Pi- Alkyl	MET542(1)	5.22
			Pi-Sigma	ALA558(1)	2.37
			Pi-Cation	ARG624 (2)	3.56, 4.25
			Pi-Anion	ASP623 (2)	3.17, 3.38
			Pi-Pi T-shaped	TYR456 (1)	5.64
			Pi-lone Pair	TYR456(1)	2.83
			Carbon Hydrogen bonds	ASP452 (1), LYS621(1)	2.56, 2.44
1,6-di-O-galloyl- beta-D-glucose (440221)	-7.5	2.9	Conventional hydrogen bonds	ASP452 (1), ASP623 (1), TYR456(1), LYS545(1), ARG555(1) THR680 (2) THR556 (2)	2.38, 2.08, 2.69, 4.42, 2.23 1.71, 2.87 2.83, 2.10
			Pi-Cation	ARG553 (1)	3.60
			Pi-Anion	ASP623 (1), ARG624 (2)	4.44, 3.79, 4.09
			Pi-Alkyl	ALA558	4.67
Pyrophephorbide A (161456)	-7.3	1.4	Conventional hydrogen bonds	ARG553 (2) THR556 (1), LYS621 (1), ASP760 (1)	2.50, 3.35 2.62, 3.11, 1.97
			Pi- Alkyl	ARG553 (1), LYS621 (1), TYR455 (2)	4.76, 4.93, 4.24, 5.25
			Alkyl	CYS622 (1), ARG554 (1), ARG553 (1)	4.61, 4.46, 3.89

		Pi-Sigma	ARG553 (1)	2.64	
		Pi-Cation	ARG553 (1), LYS621 (1)	3.37, 2.55	
		Pi-Anion	ASP623 (1)	3.28	
Pheophorbide A (253193)	-7.3	1	Conventional hydrogen bonds	ARG553 (1), ASN691 (1)	2.90, 2.08
			Alkyl	THR556 (3)	3.19, 2.56, 2.28
			Alkyl	PRO620 (1)	5.08
			Pi- Alkyl	TYR455 (1)	3.83
			Pi-Cation	ARG553 (3)	3.66, 3.67, 3.90
			Pi-Anion	ASP623 (2)	3.22, 3.51
Beta-Sitosterol (222284)	-7.0	1.5	Conventional hydrogen bonds	ALA688 (1)	2.87
			Alkyl	LYS621 (1), ARG624 (1), ALA688 (1)	5.04, 4.88, 5.31
Vitexin (5280441)	-6.5	2.4	Conventional hydrogen bonds	ARG553 (1), THR556 (1), ASP618 (1), LYS621 (1), ASP623 (1)	3.37, 2.94, 2.22, 3.11, 2.30
				TYR455 (2)	3.03, 2.80
			Pi-Cation	ARG553 (2)	4.03, 4.54
			Pi-Anion	ARG624 (1)	4.842
			Carbon Hydrogen bonds	ALA554, LYS621 (2)	2.46, 2.44, 3.30

1,6-di-O-galloyl-beta-D-glucose, a natural product found in an abundant amount in *Acacia nilotica*, has a previously reported activity on HIV-1 reverse transcriptase (RT) ²⁹. Our study demonstrated that this molecule shows a promising anti-SARS-CoV-2 polymerase activity, forming nine-strong H bonding, pi-cationic, and pi-anionic interaction with four amino acids, and pi-alkyl bond (Table 3 and Figure 4).

Pyropheophorbide A and pheophorbide A are compounds found in many plants, and they have possess a significant inhibitory activity against H1N1, H3N2, H5, and B influenza viruses ⁵⁵. Both compounds score low docking energy (-7.3) and form many types of interactions with the SARS-CoV-2 RdRp enzyme (Table 3) (Figures 5 and 6).

0000With low binding energy (-7), three alkyl bonds, and 2.87Å distanced hydrogen bond, beta-sitosterol, tightly blocked the active site of the RdRp enzyme (Table 3 and Figure 7). This good interaction aligned with a previously reported capacity of beta-sitosterol to inhibit the enzymatic activity of SARS 3CLpro ⁵⁶.

Vitexin interacts with RdRp through seven hydrogen bonds, two pi-cationic bonds, one pi-anionic bond, and two carbon-hydrogen bonds (Table 3 and Figure 8).

Three antiviral agents (velpatasvir, IDX-184, oseltamivir, and ribavirine), showed a high activity against SARS-CoV-2 RdRp. Velpatasvir is a hepatitis C RNA polymerase inhibitor ⁵⁷, that shows here, a high affinity against the SARS-CoV-2 RdRp enzyme, with -9.3 binding energy and 1.7 RMSD. Similarly, IDX-184 previously reported with activity against RdRps of HCV, MERS and SARS HCoV, and Zika virus ⁵⁸, and showed -8.8 docking energy. This finding agrees with Elfiky, (2020), who reported -9 docking energy of IDX-184 with SARS-CoV-2 RdRp ⁵⁸ (Table 3).

3.3.1. Interactions of ligands and RBD

Natural ligands showed numerous interactions with the following amino acids; THR345, ARG403, ASP405, GLN409, GLY416, LYS417, ILE418, TYR421, GLY496, TYR453,

TYR495, GLY504, and TYR505 (Table 4), these residues located at the binding site of RBD ¹. Glycyrrhizin was the most active compound on RBD that scored the lowest energy -7.3 kcal/mol and an RMSD within the acceptable range (2.3Å). Glycyrrhizin forms a strong H bonding with exposed TYR505, which has known contact with the ACE2 receptor ⁵⁹. Glycyrrhizin which creates alkyl interaction with LYS417, is one of the most important mutant residues in SARS-CoV-2 RBD ¹, which may contribute to its increased binding affinity to ACE2 receptors. In addition, glycyrrhizin interacts with another important residue (TYR453) that interacts with HIS34 of ACE2. Blocking of these important residues may interfere with the virus binding to human cells (Figure 9). Rutin created two conventional hydrogen bonds with TYR453 (ACE2 binding residue) and ILE418, located at the hydrophobic pocket of RBD ⁵⁹.

The presence of pi-alkyl and carbon-hydrogen bonds in the RBD active site make rutin the second active compound with binding energy -6.9 (Figure 10). Pheophorbide A makes a hydrogen bond with GLN409, in addition to alkyl and pi-alkyl bonds with different aliphatic amino acids in the active site of RBD (Table 4) (Figure 11).

Table 4. Interaction of active compounds with SARS-CoV-2 RBD (6VSB) and Human ACE2 receptor (6VW1).

Compounds (PubChem ID)	RBD			ACE2	
	Type of interaction	Amino acid residues (No. of bonds)	Distance (Å)	Amino acid residues (No. of bonds)	Distance (Å)
Glycyrrhizin (14982)	Conventional hydrogen bonds	TYR505 (1)	3.31	ASP350 (1)	2.71
	Alkyl	LYS417 (1)	4.85	LEU391(1), ALA99(1), LEU100(1)	4.96, 4.35, 4.68
	Carbon hydrogen bond	GLY496 (2)	2.76, 3.08	ALA99(1)	2,54
	Pi- Alkyl	TYR453, TYR495	4.18, 5.13	LEU391(1), ARG393 (2)	4.97
	Pi-Pi Stacked	-	-	PHE40(1)	5.49
Rutin (5280805)	Conventional hydrogen bonds	TYR453 (1), ILE418(1),	2.70, 2.73	ASP30 (2), ARG393 (2), ASN33(1)	2.31, 2.94, 2.20, 2.43, 2.96
	Pi-Alkyl	TYR421 (1), ARG403 (2)	5.25, 4.37, 4.97	PRO389	4.94
	Carbon Hydrogen bond	GLY416(1)	3.58	GLN388, ALA387	2.50, 2.53
	Pi-Sigma	-	-	PRO389	2.48
	Alkyl	-	-	ALA386, PPRO389	4.22
Pheophorbide A (253193)	Conventional hydrogen bonds	GLN409(1)	3.19	ARG393 (2), ASP30	2.03, 3.07, 2.0
	Alkyl	ILE418 (1)	5.18	VAL93,AL A387, LEU29	5.11, 4.48, 4.94
	Pi- Alkyl	TYR505 (1) (1), ARG403 (2), TYR453(1), TYR495(1), ILE418(1)	5.41, 4.71, 5.08, 4.30, 5.06, 5.18	PRO389 (2)	5.36, 5.27
	Amide-Pi Stacked	ASP405(1), GLY504 (2)	5.05, 4.80, 5.41		

3.3.2. Interactions of ligands and ACE2 receptor

Several studies have reported that SARS-CoV-2 enters its target cells through angiotensin-converting enzyme 2 (ACE2)^{60,61}. ACE2 is highly expressed in the mouth and tongue, which facilitates the entry of the virus into the body⁶⁰. The blocking of the ACE2 receptor could reduce its binding affinity to viral spike protein attachment. We identified three compounds (glycyrrhizin, rutin, and pheophorbide A), with a high binding affinity (-7.8, -6.9, and -6.5

kcal/mol, respectively) to the ACE2 receptor. These compounds created an interaction with the following residues: PHE4, LEU29, ASP30, ASN33, VAL93, ALA99, LEU100, ALA387, ASP350, ALA387, GLN388,

PRO389, LEU391, and ARG393. Some of them (such as ASP30) have an essential role in RBD binding ^{50,62} (Table 4) (Figures 12, 13, and 14).

3.4. Predicted ADMET profiles of compounds

Beta-sitosterol, pheophorbide A, and pyropheophorbide A are of high (more than 95%) human intestinal absorption (HIA) values, which indicates their high absorbance rate in the human intestinal tract. They also showed high permeability to Caco-2 (cells derived from a colon cancer cell) and MDCK (cells derived from canine kidney cells) cell models when compared with antiviral drugs (velpatasvir, IDX-184, and oseltamivir). Rutin and 6-Bis-O-galloyl-beta-D-glucose show the lowest intestinal absorption rate (less than 7%), indicating their reduced intestinal absorption rate. This finding agrees with previous clinical studies that show the low absorption rate of rutin ^{63,64} (Table 5).

Drug distribution depends on a drug's ability to penetrate the blood-brain barrier (BBB), as well as its degree of plasma protein binding (PPB) ⁶⁵. Most of our compounds, as predicted by PreADMET, have a high binding affinity to plasma protein (up to 100%), and good penetration of the BB, compared with reference antiviral agents (Table 5).

Table 5. ADMET predicted profile of top eight natural compounds as compared to three reference antiviral molecules

Aadme	Natural compounds								References antiviral compounds		
	1,6-Bis-O-galloyl-beta-D-glucose	beta-Sitosterol	Rutin	Pheophorbide A	Pyropheophorbide A	Glycyrrhizin	Baicalin	Vitexin	Velpatasvir	IDX-184	Oseltamivir
Absorption											
HIA (%)	2,65	100	2,86	96,15	95,66	9,46	32,42	31,37	92,72	26,39	87,16
Caco2 (mm/sec)	6,9455	52,3734	7,9127	21,1468	22,0961	20,7977	11,5594	5,49	23,86	0,6315	14,12
MDCK (mm/sec)	0,4922	8,8572*	0,3269	0,0434*	0,0439	0,0434*	0,1478	0,54	0,043	0,044	5,028
Pgp inhibition	Non	Inhibitor	Non	Non	Inhibitor	Non	Non	Non	Inhibitor	Non	Non
Distribution											
BBB (%)	0,0313	19,8883	0,0286*	0,0337	0,3105	0,0365*	0,0252	0,039	0,2710	0,069	0,123
Plasma Protein Binding (%)	86,2074	100	43,8979	87,2730	88,0027	82,4843	75,6919	61,32	88,7939	36,8052	37,83
Metabolism											
CYP_2C19_inhibition	Inhibitor	Non	Inhibitor	Non	Non	Non	Non	Inhibitor	Non	Non	Non
CYP_2C9_inhibition	Inhibitor	Inhibitor	Inhibitor	Non	Non	Inhibitor	Inhibitor	Inhibitor	Inhibitor	Non	Non
CYP_2D6_inhibition	Non	Non	Non	Non	Non	Non	Non	Non	Non	Non	Inhibitor
CYP_2D6_substrate	Non	Non	Non	Non	Non	Non	Non	Non	Non	Non	Substrate
CYP_3A4_inhibition	Inhibitor	Inhibitor	Inhibitor	Inhibitor	Inhibitor	Inhibitor	Inhibitor	Inhibitor	Inhibitor	Inhibitor	Non
CYP_3A4_substrate	Weakly	Substrate	Weakly	Substrate	Substrate	Substrate	Weakly	Weakly	Substrate	Substrate	Weakly
Bioavailability											
Buffer solubility(mg/L)	129005	1,8010	28,8864	0,0951	0,0296	173820	77684	196,168	0,1263	3,9685**	1204,74
Pure water solubility(mg/L)	8527,4	0,0015	217,2070	0,3530	0,2631	0,0555	361,9440	344,563	0,0000	6,6251	2517,58
Skin Permeability	-4,3906	-0,5934	-4,6667	-3,3780	-3,4464	-1,8968*	-4,3741	-4,611	-3,0823*	-2,9751*	-3,3491

Toxicity assays											
Algae at	0,0009	0,0072	0,0070	0,0020	0,0035	0,0003	0,0192	0.029	0,0001	0,0044	0,0817
Ames test	non-mutagen	mutagen	non-mutagen	mutagen	mutagen	non-mutagen	mutagen	non-mutagen	mutagen	non-mutagen	mutagen
Carcino Mouse	positive	negative	positive	positive	positive	positive	negative	positive	negative	negative	negative
Carcino Rat	negative	negative	negative	positive	positive	positive	positive	negative	negative	negative	negative
Daphnia at	0,0027	0,4737	2,5526	0,0060	0,0045	0,1218	0,3948	0,78	0,0009	0,4436	0,4499
hERG inhibition	Low risk	ambiguous	ambiguous	Low risk	ambiguous	ambiguous	ambiguous	High risk	High risk	ambiguous	Low risk

The cytochrome P450 (CYP) enzymes play a major role in the first phase of drug metabolism and detoxification of harmful substances in cells, such as drugs and toxins⁶⁶. Inhibition of CYP enzymes could lead to toxic side effects or a decrease in drug effectiveness⁶⁷. Pheophorbide A, and pyropheophorbide A showed low toxicity to CYP enzymes, followed by glycyrrhizin, beta-Sitosterol, baicalin, and vitexin, which were inhibitors for two of six CYP enzymes predicted by PreADMET. 1, 6-Bis-O-galloyl-beta-D-glucose and rutin show the highest inhibitory effect for CYP enzymes. The inhibitory effect of rutin to CYP3A4 is in agreement with a previous study that found that rutin is one of the most potent CYP3A4 inhibitors⁶⁶ (Table 5).

Four compounds (1, 6-Bis-O-galloyl-beta-D-glucose, glycyrrhizin, rutin, and vitexin) were predicted by the Ames test to have no carcinogenicity and mutagenicity.

Conclusion

The discovery and development of novel anti-SARS-CoV-2 drugs to fight the global pandemic is of worldwide urgency. In this study, we discovered eight potential SARS-CoV-2 inhibitors (glycyrrhizin, rutin, baicalin, 1, 6-di-O-galloyl-beta-D-glucose, pyropheophorbide A, pheophorbide A, beta-Sitosterol, and vitexin). These outcomes indicate that these compounds are potential candidates to be utilized in lead optimization for the development of anti-SARS-CoV-2 drugs.

Declarations

Funding

This project was funded by the Deanship of Scientific Research (DSR), King Abdulaziz University, Jeddah, Kingdom of Saudi Arabia under grant No (D-658-130-1441)

Conflicts of interest

None of the authors has financial interests or conflicts of interest related to this research

Acknowledgement

The authors thanks [LetPub](#) and [Hassuna Altayeb](#) from Al Ittihad Newspaper for their free language editing service.

Authors' contributions

HNA, LB, KC and MAZ designed the study, NHA and KC performed the docking study, HNA, LB, KC, OSB and MAZ wrote the manuscript, all the authors approved the final version of the manuscript.

References

- Zhu, N. *et al.* A novel coronavirus from patients with pneumonia in China, 2019. *New England Journal of Medicine* (2020).

- 2 WHO. Novel Coronavirus-China. <https://www.who.int/csr/don/12-january-2020-novel-coronavirus-china/en/>. Accessed 1 Feb 2020. (2020).
- 3 Weiss, S. R. & Leibowitz, J. L. in *Advances in virus research* Vol. 81 85-164 (Elsevier, 2011).
- 4 Su, S. *et al.* Epidemiology, genetic recombination, and pathogenesis of coronaviruses. *Trends in microbiology* **24**, 490-502 (2016).
- 5 Drosten, C. *et al.* Identification of a novel coronavirus in patients with severe acute respiratory syndrome. *New England journal of medicine* **348**, 1967-1976 (2003).
- 6 Zhong, N. *et al.* Epidemiology and cause of severe acute respiratory syndrome (SARS) in Guangdong, People's Republic of China, in February, 2003. *The Lancet* **362**, 1353-1358 (2003).
- 7 Zaki, A. M., Van Boheemen, S., Bestebroer, T. M., Osterhaus, A. D. & Fouchier, R. A. Isolation of a novel coronavirus from a man with pneumonia in Saudi Arabia. *New England Journal of Medicine* **367**, 1814-1820 (2012).
- 8 Kampf, G., Todt, D., Pfaender, S. & Steinmann, E. Persistence of coronaviruses on inanimate surfaces and its inactivation with biocidal agents. *Journal of Hospital Infection* (2020).
- 9 Chappell, M. C., Pirro, N. T., Sykes, A. & Ferrario, C. M. Metabolism of angiotensin-(1-7) by angiotensin-converting enzyme. *Hypertension* **31**, 362-367 (1998).
- 10 Keidar, S., Kaplan, M. & Gamliel-Lazarovich, A. ACE2 of the heart: from angiotensin I to angiotensin (1-7). *Cardiovascular research* **73**, 463-469 (2007).
- 11 Epelman, S. *et al.* Detection of soluble angiotensin-converting enzyme 2 in heart failure: insights into the endogenous counter-regulatory pathway of the renin-angiotensin-aldosterone system. *Journal of the American College of Cardiology* **52**, 750-754 (2008).
- 12 Kemp, B. A. *et al.* AT2 receptor activation prevents sodium retention and reduces blood pressure in angiotensin II-dependent hypertension. *Circulation research* **119**, 532-543 (2016).
- 13 De Jongh, R., De Backer, W., Mohan, R., Jorens, P. & van Overveld, F. Angiotensin-converting enzyme activity in serum and bronchoalveolar lavage fluid after damage to the alveolo-capillary barrier in the human lung. *Intensive care medicine* **19**, 390-394 (1993).
- 14 Warner, F. J. *et al.* Angiotensin-converting enzyme 2 (ACE2), but not ACE, is preferentially localized to the apical surface of polarized kidney cells. *Journal of Biological Chemistry* **280**, 39353-39362 (2005).
- 15 Yan, R. *et al.* Structural basis for the recognition of SARS-CoV-2 by full-length human ACE2. *Science* **367**, 1444-1448 (2020).
- 16 Peng, C. *et al.* Exploring the Binding Mechanism and Accessible Angle of SARS-CoV-2 Spike and ACE2 by Molecular Dynamics Simulation and Free Energy Calculation. *Preprint*. <https://doi.org/10.26434/chemrxiv.11877492>, v1 (2020).
- 17 Wrapp, D. *et al.* Cryo-EM structure of the 2019-nCoV spike in the prefusion conformation. *Science* **367**, 1260-1263 (2020).
- 18 Walls, A. C. *et al.* Structure, function, and antigenicity of the SARS-CoV-2 spike glycoprotein. *Cell* (2020).
- 19 Kuba, K. *et al.* A crucial role of angiotensin converting enzyme 2 (ACE2) in SARS coronavirus-induced lung injury. *Nature medicine* **11**, 875-879 (2005).
- 20 Gordon, D. E. *et al.* A SARS-CoV-2-human protein-protein interaction map reveals drug targets and potential drug-repurposing. *BioRxiv* (2020).
- 21 Chen, L., Xiong, J., Bao, L. & Shi, Y. Convalescent plasma as a potential therapy for COVID-19. *The Lancet Infectious Diseases* (2020).
- 22 Aguiar, A. C. *et al.* Chloroquine analogs as antimalarial candidates with potent in vitro and in vivo activity. *International Journal for Parasitology: Drugs and Drug Resistance* **8**, 459-464 (2018).
- 23 Savarino, A., Boelaert, J. R., Cassone, A., Majori, G. & Cauda, R. Effects of chloroquine on viral infections: an old drug against today's diseases. *The Lancet infectious diseases* **3**, 722-727 (2003).
- 24 Vincent, M. J. *et al.* Chloroquine is a potent inhibitor of SARS coronavirus infection and spread. *Virology journal* **2**, 69 (2005).
- 25 Wang, M. *et al.* Remdesivir and chloroquine effectively inhibit the recently emerged novel coronavirus (2019-nCoV) in vitro. *Cell research* **30**, 269-271 (2020).
- 26 Holshue, M. L. *et al.* First case of 2019 novel coronavirus in the United States. *New England Journal of Medicine* (2020).
- 27 Agostini, M. L. *et al.* Coronavirus susceptibility to the antiviral remdesivir (GS-5734) is mediated by the viral polymerase and the proofreading exonuclease. *MBio* **9**, e00221-00218 (2018).

- 28 Rehman, S., Ashfaq, U. A., Riaz, S., Javed, T. & Riazuddin, S. Antiviral activity of *Acacia nilotica* against Hepatitis C Virus in liver infected cells. *Virology journal* **8**, 220 (2011).
- 29 Chinsembu, K. C. Chemical diversity and activity profiles of HIV-1 reverse transcriptase inhibitors from plants. *Revista Brasileira de Farmacognosia* (2019).
- 30 Umar, S. *et al.* Protective and antiviral activities of *Nigella sativa* against avian influenza (H9N2) in turkeys. *J. Saudi Soc. agric. Sci* (2016).
- 31 Bouslama, L., Kouidhi, B., Alqurashi, Y. M., Chaieb, K. & Papetti, A. Virucidal Effect of Guggulsterone Isolated from *Commiphora gileadensis*. *Planta medica* **85**, 1225-1232 (2019).
- 32 Al-Bagieh, N. Antiherpes simplex virus type 1 activity of benzylisothiocyanate. *Biomedical letters* **47**, 67-70 (1992).
- 33 Benzekri, R. *et al.* Anti HSV-2 activity of *Peganum harmala* (L.) and isolation of the active compound. *Microbial pathogenesis* **114**, 291-298 (2018).
- 34 Li, S.-y. *et al.* Identification of natural compounds with antiviral activities against SARS-associated coronavirus. *Antiviral research* **67**, 18-23 (2005).
- 35 Tragoolpua, Y. & Jatisatienr, A. Anti-herpes simplex virus activities of *Eugenia caryophyllus* (Spreng.) Bullock & SG Harrison and essential oil, eugenol. *Phytotherapy Research: An International Journal Devoted to Pharmacological and Toxicological Evaluation of Natural Product Derivatives* **21**, 1153-1158 (2007).
- 36 Chen, F. *et al.* In vitro susceptibility of 10 clinical isolates of SARS coronavirus to selected antiviral compounds. *Journal of Clinical Virology* **31**, 69-75, doi:<https://doi.org/10.1016/j.jcv.2004.03.003> (2004).
- 37 Yang, Y., Xiu, J., Zhang, L., Qin, C. & Liu, J. Antiviral activity of punicalagin toward human enterovirus 71 in vitro and in vivo. *Phytomedicine* **20**, 67-70 (2012).
- 38 Li, Z. *et al.* Natural Sulforaphane From Broccoli Seeds Against Influenza A Virus Replication in MDCK Cells. *Natural Product Communications* **14**, 1934578X19858221 (2019).
- 39 Elizondo-Gonzalez, R. *et al.* In vitro characterization of the antiviral activity of fucoidan from *Cladosiphon okamuranus* against Newcastle Disease Virus. *Virology journal* **9**, 307 (2012).
- 40 Wang, Z. *et al.* Discovery and SAR Research for Antivirus Activity of Novel Butenolide on Influenza A Virus H1N1 In Vitro and In Vivo. *ACS omega* **4**, 13265-13269 (2019).
- 41 Shahzad, A. & Cohrs, R. J. In vitro antiviral activity of honey against varicella zoster virus (VZV): a translational medicine study for potential remedy for shingles. *Translational biomedicine* **3** (2012).
- 42 Watanabe, K., Rahmasari, R., Matsunaga, A., Haruyama, T. & Kobayashi, N. Anti-influenza viral effects of honey in vitro: potent high activity of manuka honey. *Archives of medical research* **45**, 359-365 (2014).
- 43 Berman, H. M. *et al.* The protein data bank. *Acta Crystallographica Section D: Biological Crystallography* **58**, 899-907 (2002).
- 44 Kim, S. *et al.* PubChem substance and compound databases. *Nucleic acids research* **44**, D1202-D1213 (2016).
- 45 Yusuf, D., Davis, A. M., Kleywegt, G. J. & Schmitt, S. An alternative method for the evaluation of docking performance: RSR vs RMSD. *Journal of chemical information and modeling* **48**, 1411-1422 (2008).
- 46 Neira, J. L. *et al.* Identification of a drug targeting an intrinsically disordered protein involved in pancreatic adenocarcinoma. *Scientific reports* **7**, 1-15 (2017).
- 47 Rashid, M. Design, Synthesis and ADMET prediction of Bis-benzimidazole as Anticancer agent. *Bioorganic Chemistry*, 103576 (2020).
- 48 Makhaeva, G. F. *et al.* Synthesis, molecular docking, and biological evaluation of 3-oxo-2-tolylhydrazinylidene-4, 4, 4-trifluorobutanoates bearing higher and natural alcohol moieties as new selective carboxylesterase inhibitors. *Bioorganic chemistry* **91**, 103097 (2019).
- 49 Arora, R., Issar, U. & Kakkar, R. Identification of novel urease inhibitors: pharmacophore modeling, virtual screening and molecular docking studies. *Journal of Biomolecular Structure and Dynamics* **37**, 4312-4326 (2019).
- 50 Yan, R. *et al.* Structural basis for the recognition of the SARS-CoV-2 by full-length human ACE2. *Science* (2020).
- 51 Ding, Y. *et al.* Assessing the similarity of ligand binding conformations with the contact mode score. *Computational biology and chemistry* **64**, 403-413 (2016).
- 52 Cinatl, J. *et al.* Glycyrrhizin, an active component of liquorice roots, and replication of SARS-associated coronavirus. *The Lancet* **361**, 2045-2046 (2003).

- 53 Wang, L., Yang, R., Yuan, B., Liu, Y. & Liu, C. The antiviral and antimicrobial activities of licorice, a widely-used Chinese herb. *Acta Pharmaceutica Sinica B* **5**, 310-315 (2015).
- 54 Zhang, L. & Zhou, R. Binding Mechanism of Remdesivir to SARS-CoV-2 RNA Dependent RNA Polymerase. (2020).
- 55 Nerome, K. *et al.* Functional growth inhibition of influenza A and B viruses by liquid and powder components of leaves from the subtropical plant *Melia azedarach* L. *Archives of virology* **163**, 2099-2109 (2018).
- 56 Yang, Y., Islam, M. S., Wang, J., Li, Y. & Chen, X. Traditional Chinese Medicine in the Treatment of Patients Infected with 2019-New Coronavirus (SARS-CoV-2): A Review and Perspective. *Int J Biol Sci* **16**, 1708-1717 (2020).
- 57 Ju, J. *et al.* Nucleotide Analogues as Inhibitors of SARS-CoV Polymerase. *bioRxiv* (2020).
- 58 Elfiky, A. A. Anti-HCV, nucleotide inhibitors, repurposing against COVID-19. *Life sciences*, 117477 (2020).
- 59 Senathilake, K., Samarakoon, S. & Tennekoon, K. Virtual Screening of Inhibitors Against Spike Glycoprotein of 2019 Novel Corona Virus: A Drug Repurposing Approach. (2020).
- 60 Hoffmann, M. *et al.* SARS-CoV-2 cell entry depends on ACE2 and TMPRSS2 and is blocked by a clinically proven protease inhibitor. *Cell* (2020).
- 61 Perico, L., Benigni, A. & Remuzzi, G. Should COVID-19 Concern Nephrologists? Why and to What Extent? The Emerging Impasse of Angiotensin Blockade. *Nephron*, 1-9 (2020).
- 62 Jamal, S. *et al.* Molecular Analyses of Over Hundred Sixty Clinical Isolates of SARS-CoV-2: Insights on Likely Origin, Evolution and Spread, and Possible Intervention. (2020).
- 63 Zhang, X. *et al.* Absorption and metabolism characteristics of rutin in Caco-2 cells. *The Scientific World Journal* **2013** (2013).
- 64 Andlauer, W., Stumpf, C. & Furst, P. Intestinal absorption of rutin in free and conjugated forms. *Biochemical pharmacology* **62**, 369-374, doi:10.1016/s0006-2952(01)00638-4 (2001).
- 65 Smith, Q. R., Fisher, C. & Allen, D. D. in *Blood–Brain Barrier* 311-321 (Springer, 2001).
- 66 Ashour, M. L., Youssef, F. S., Gad, H. A. & Wink, M. Inhibition of cytochrome P450 (CYP3A4) activity by extracts from 57 plants used in traditional chinese medicine (TCM). *Pharmacognosy magazine* **13**, 300 (2017).
- 67 Pang, X. *et al.* Screening of cytochrome P450 3A4 inhibitors via in silico and in vitro approaches. *RSC advances* **8**, 34783-34792 (2018).

Figures

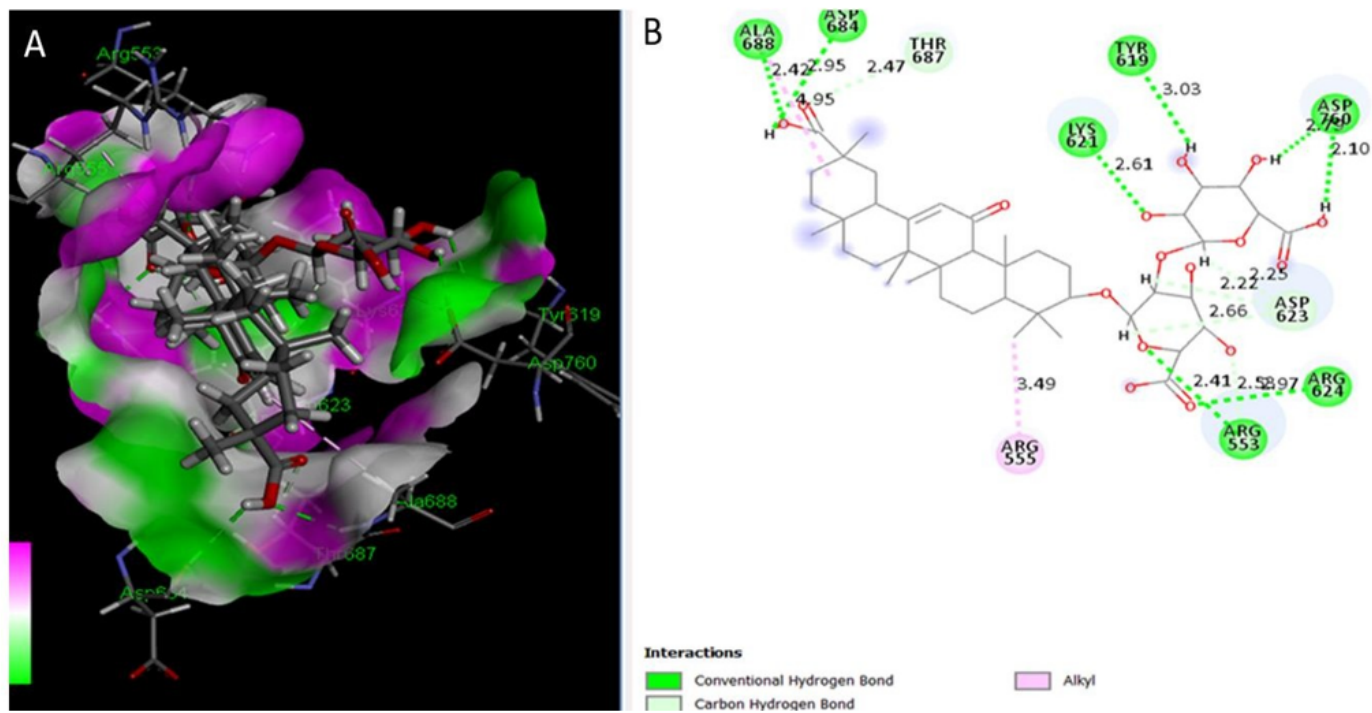


Figure 1
 Three and two-dimensional interaction of glycyrrhizin ligand with RdRp enzyme. A. Display of the receptor surfaces with H-bond contacts. B. 2D structure shows the ligand surrounded by active site residues, bond types, and distances.

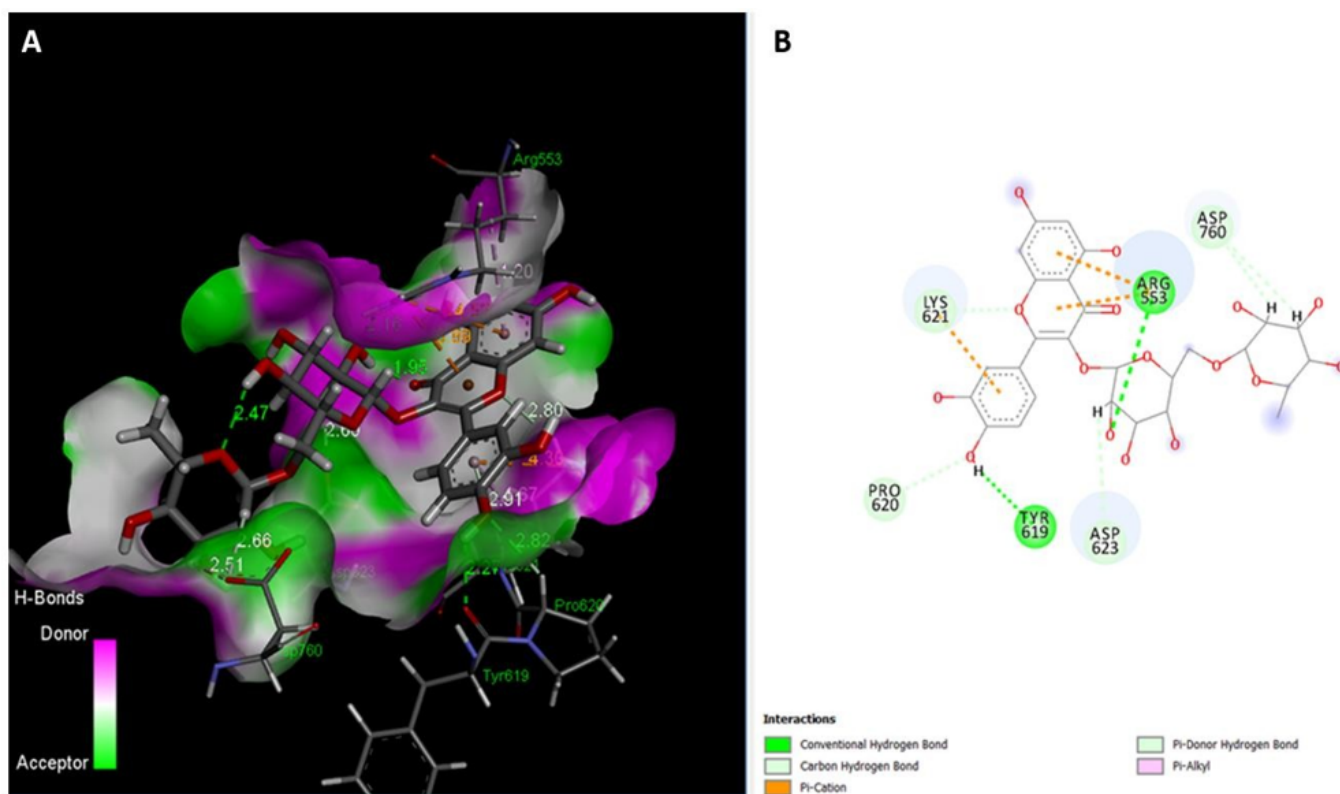


Figure 2

Three and two-dimensional interaction of rutin ligand with RdRp enzyme. A. Display of the receptor surfaces with H-bond contacts. B. 2D structure shows the ligand surrounded by active site residues, bond types, and distances.

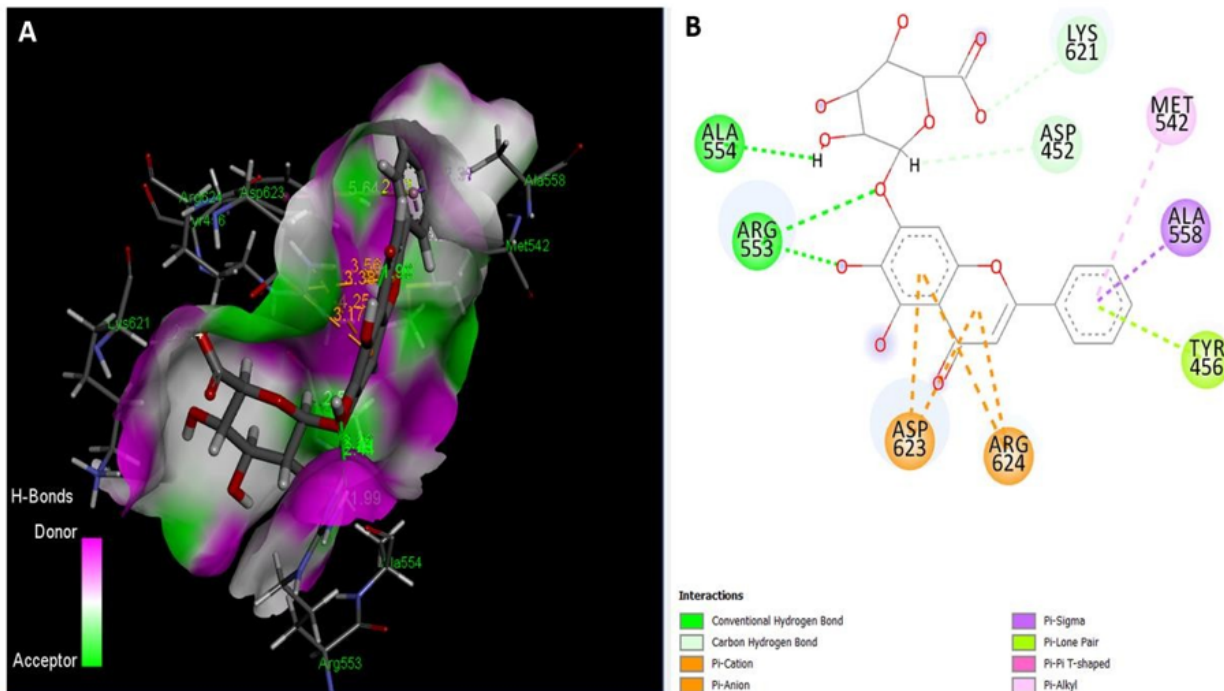


Figure 3

Three and two-dimensional interaction of baicalin ligand with RdRp enzyme. A. Display of the receptor surfaces with H-bond contacts. B. 2D structure shows the ligand surrounded by active site residues, bond types, and distances.

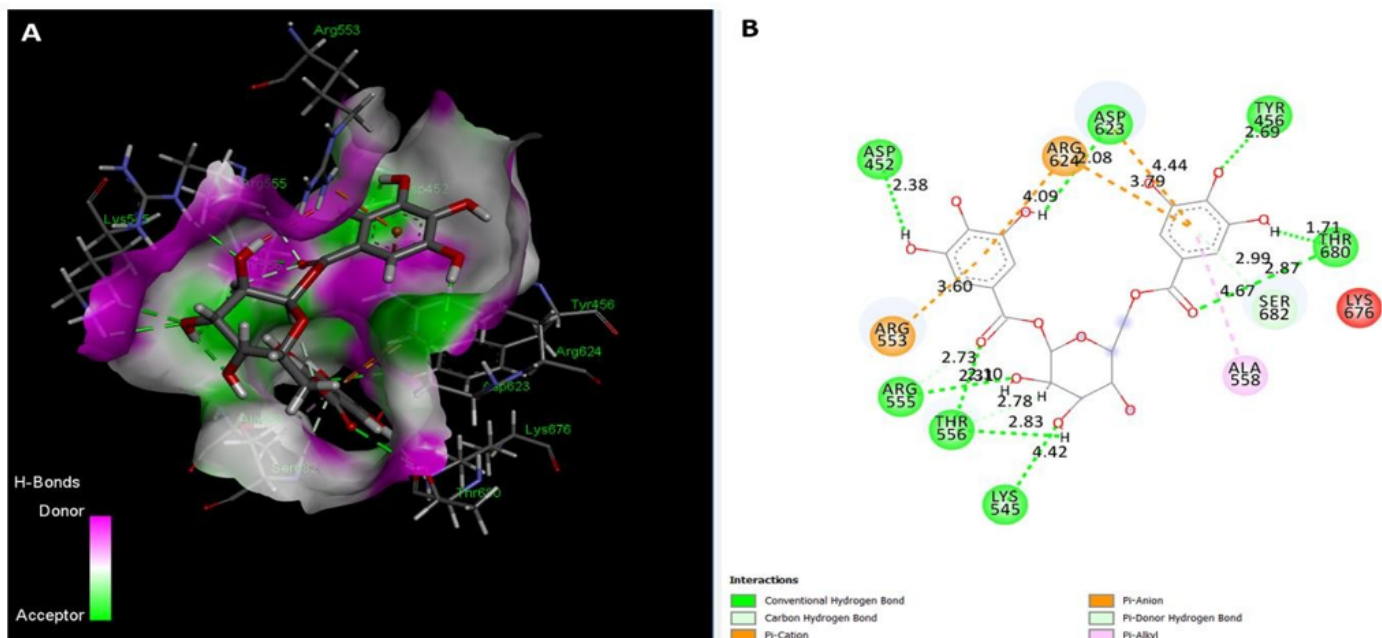


Figure 4

Three and two-dimensional interaction of 1, 6-di-O-galloyl-beta-D-glucose (ID 440221) ligand with RdRp enzyme. A. Display of the receptor surfaces with H-bond contacts. B. 2D structure shows ligand surrounded by active site residues, bond types, and distances.

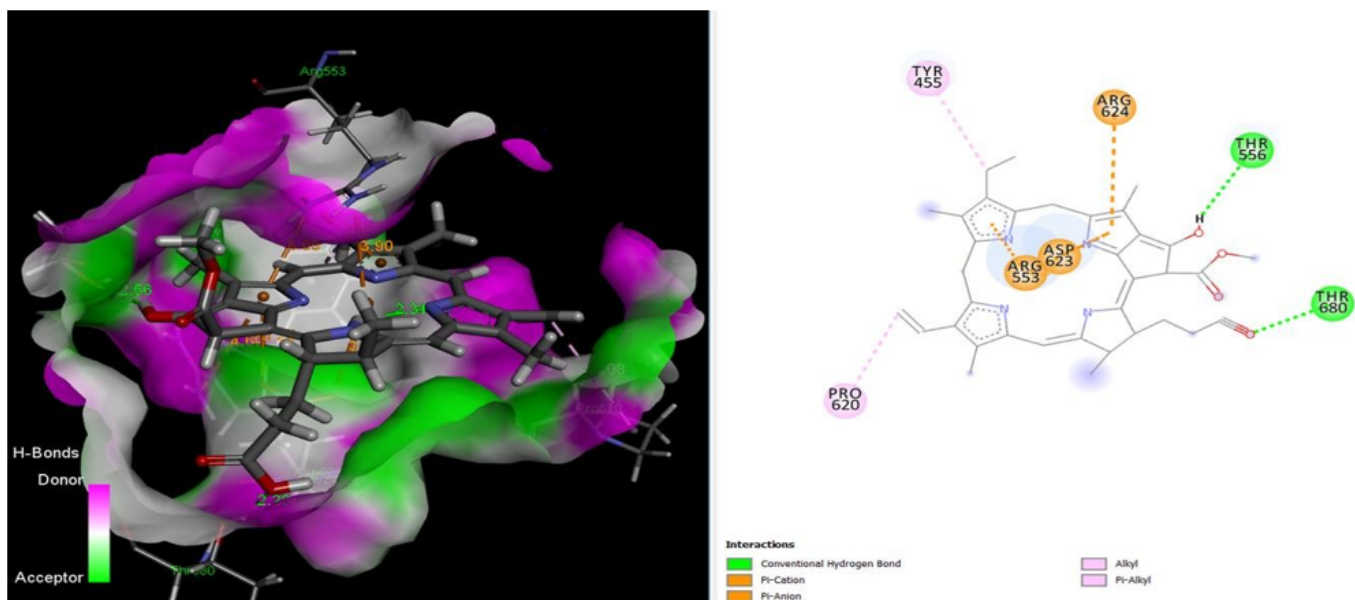


Figure 5

Three and two-dimensional interaction of pheophorbide a ligand with RdRp enzyme. A. Display of the receptor surfaces with H-bond contacts. B. 2D structure shows the ligand surrounded by active site residues, bond types, and distances.

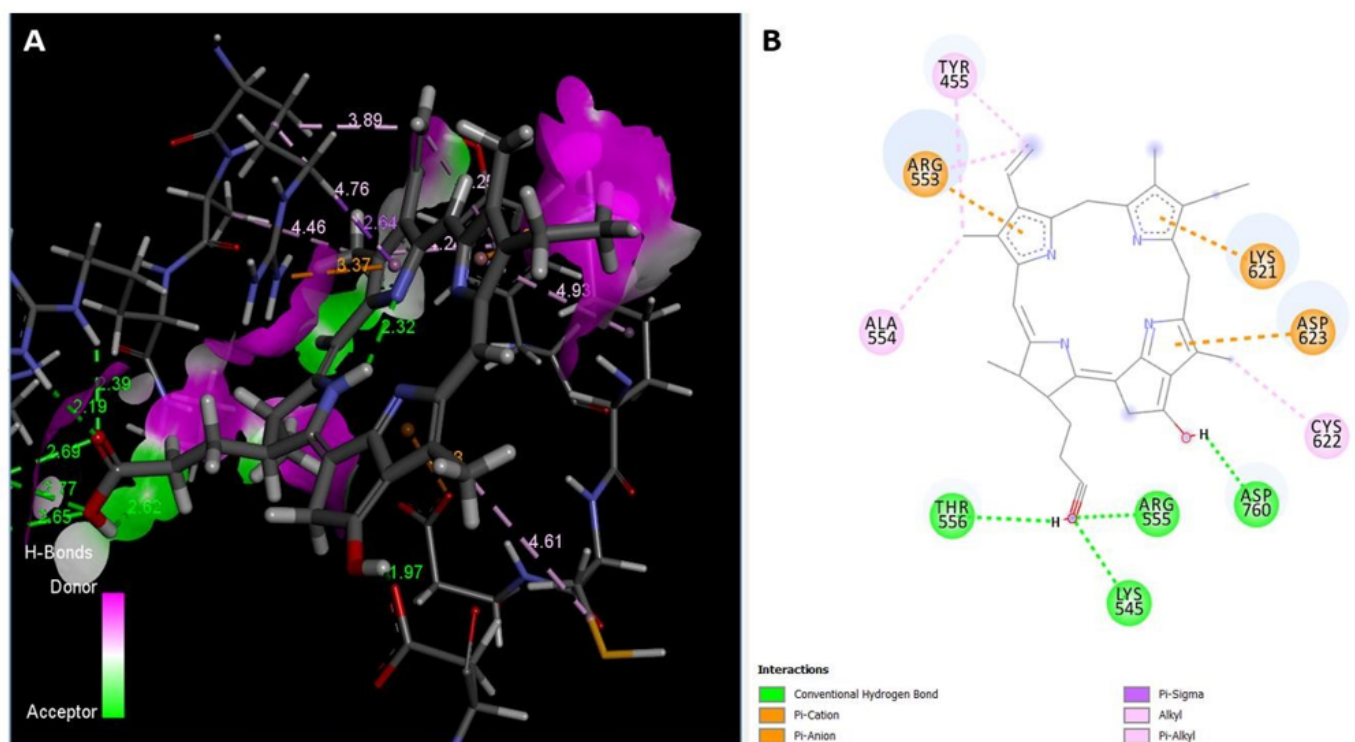


Figure 6

Three and two-dimensional interaction of pyropheophorbide A ligand with RdRp enzyme. A. Display of the receptor surfaces with H-bond contacts. B. 2D structure shows the ligand surrounded by active site residues, bond types, and distances.

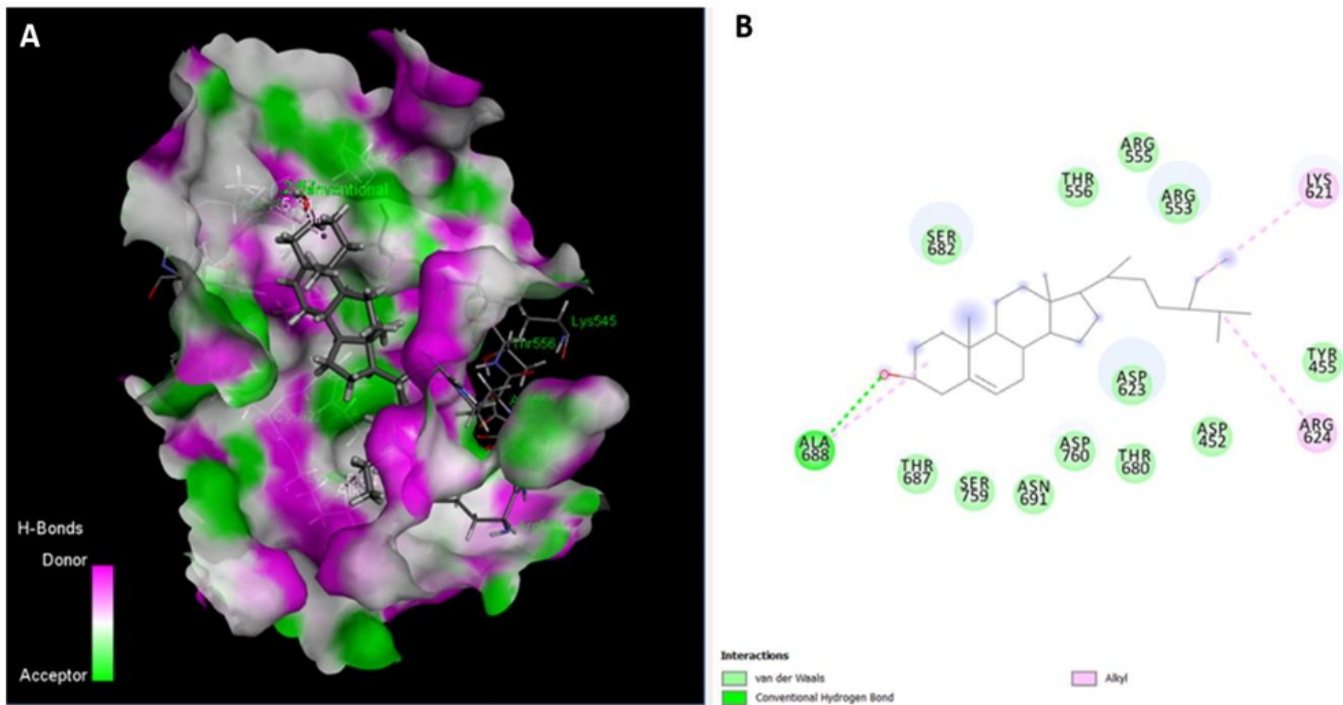


Figure 7

Three and two-dimensional interaction of beta-Sitosterol ligand with RdRp enzyme. A. Display of the receptor surfaces with H-bond contacts. B. 2D structure shows the ligand surrounded by active site residues, bonds types, and distances.

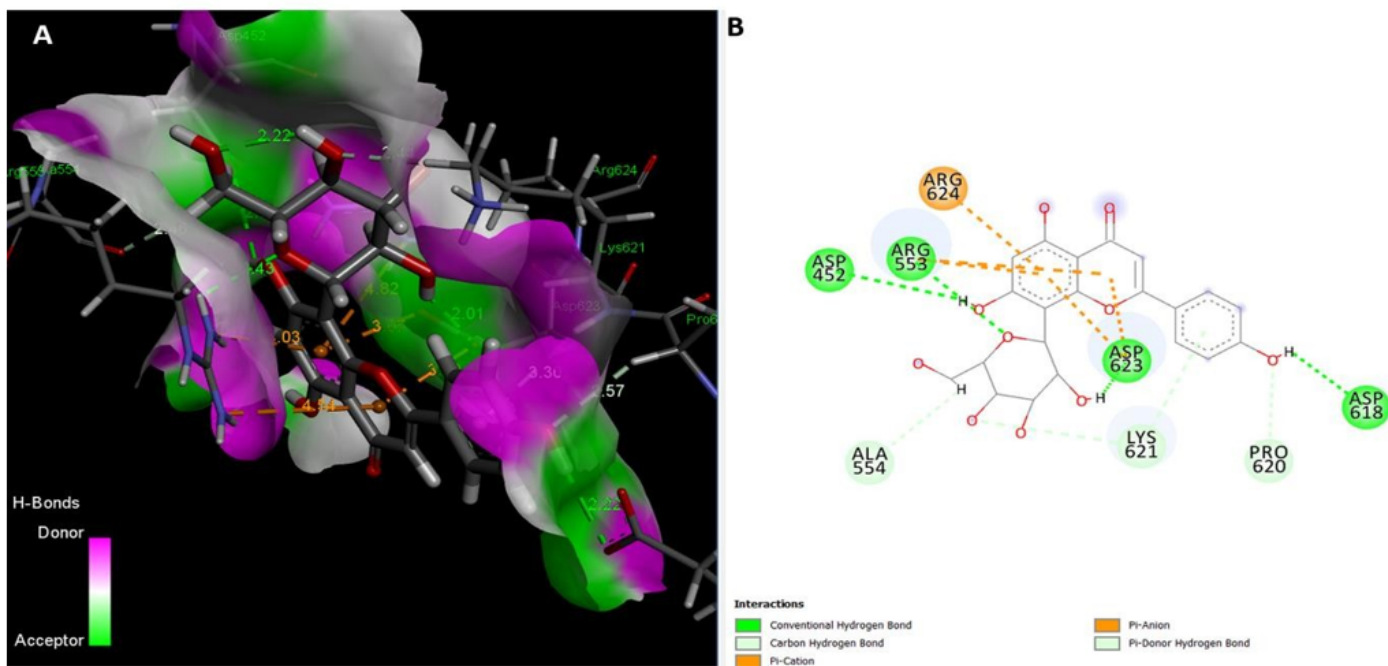


Figure 8

Three and two-dimensional interaction of vitexin ligand with RdRp enzyme. A. Display of the receptor surfaces with H-bond contacts. B. 2D structure shows the ligand surrounded by active site residues, bond types, and distances.

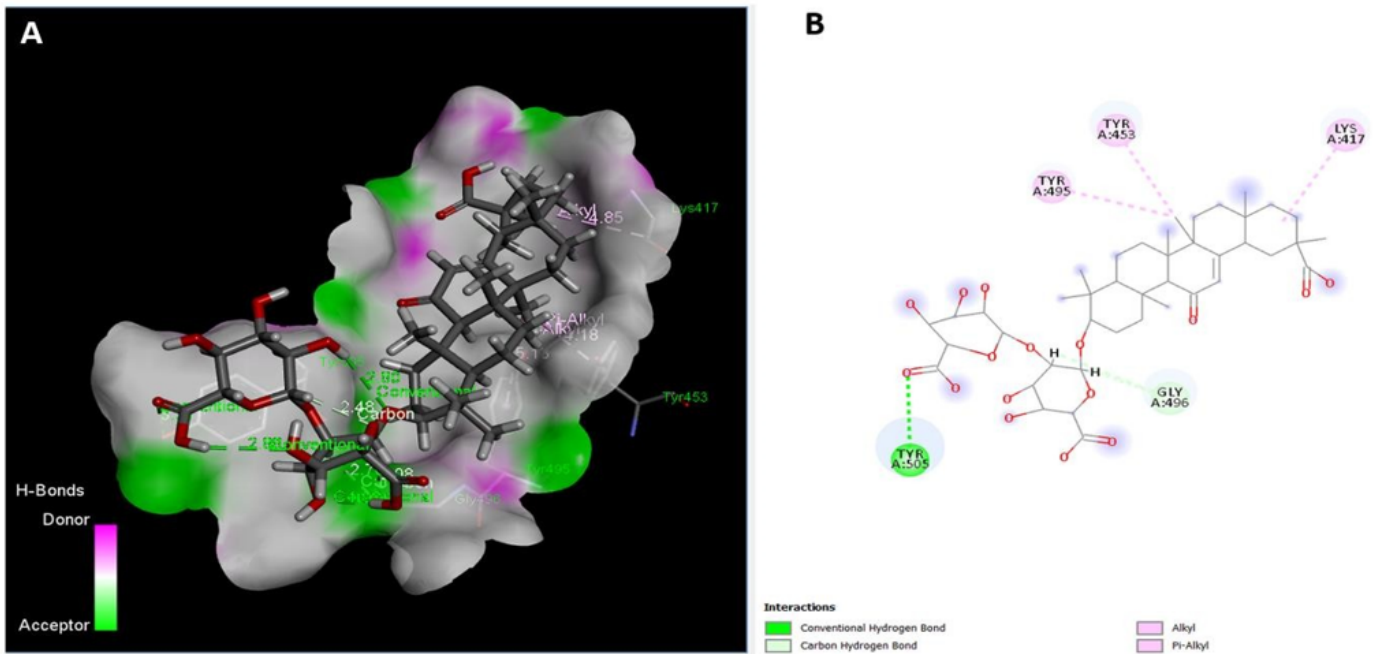


Figure 9

Three and two-dimensional interaction of glycyrrhizin ligand with Spike protein RBD. A. Display of the receptor surface with H-bond contacts. B. 2D structure shows the ligand surrounded by active site residues, bond types, and distances.

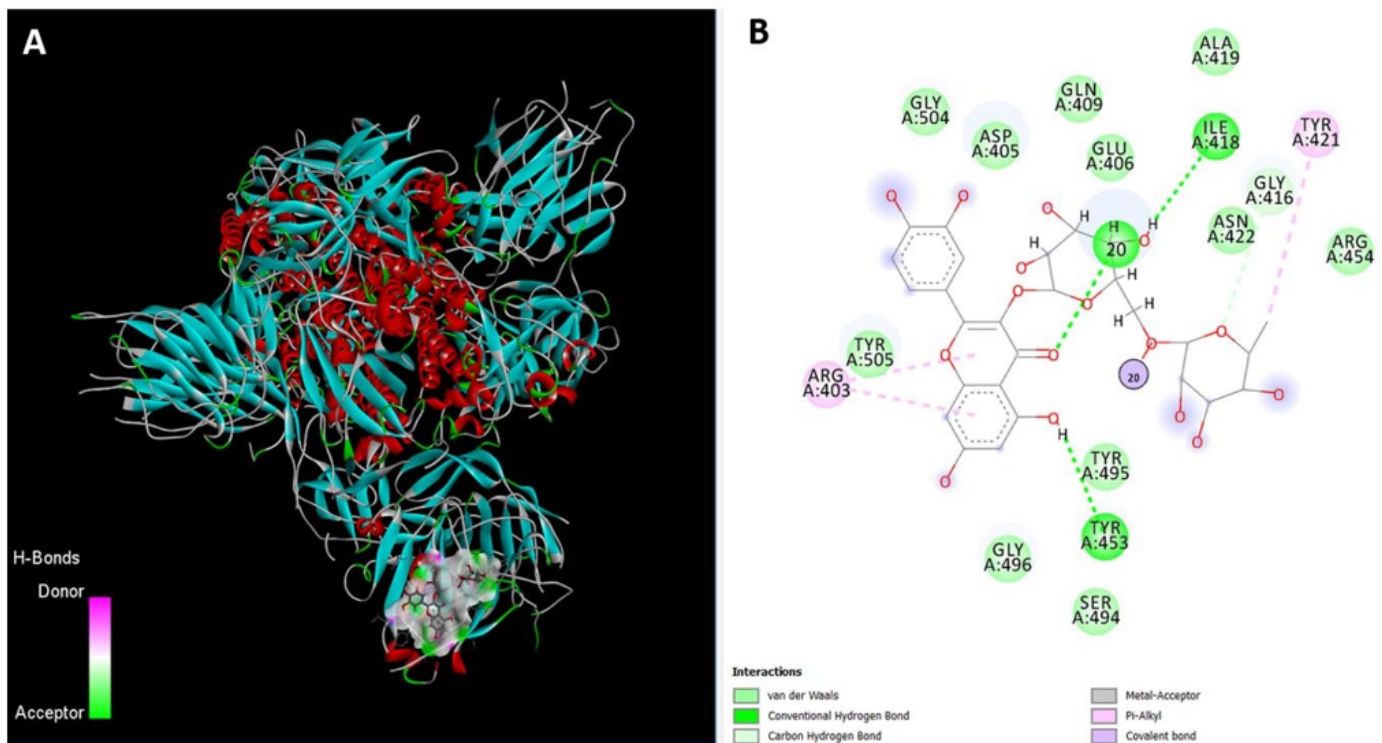


Figure 10

Three and two-dimensional interaction of rutin ligand with Spike protein RBD. A. Complete structure of spike protein, showing binding of Rutin RBD. B. 2D structure shows the ligand surrounded by active site residues, bond types, and distances.

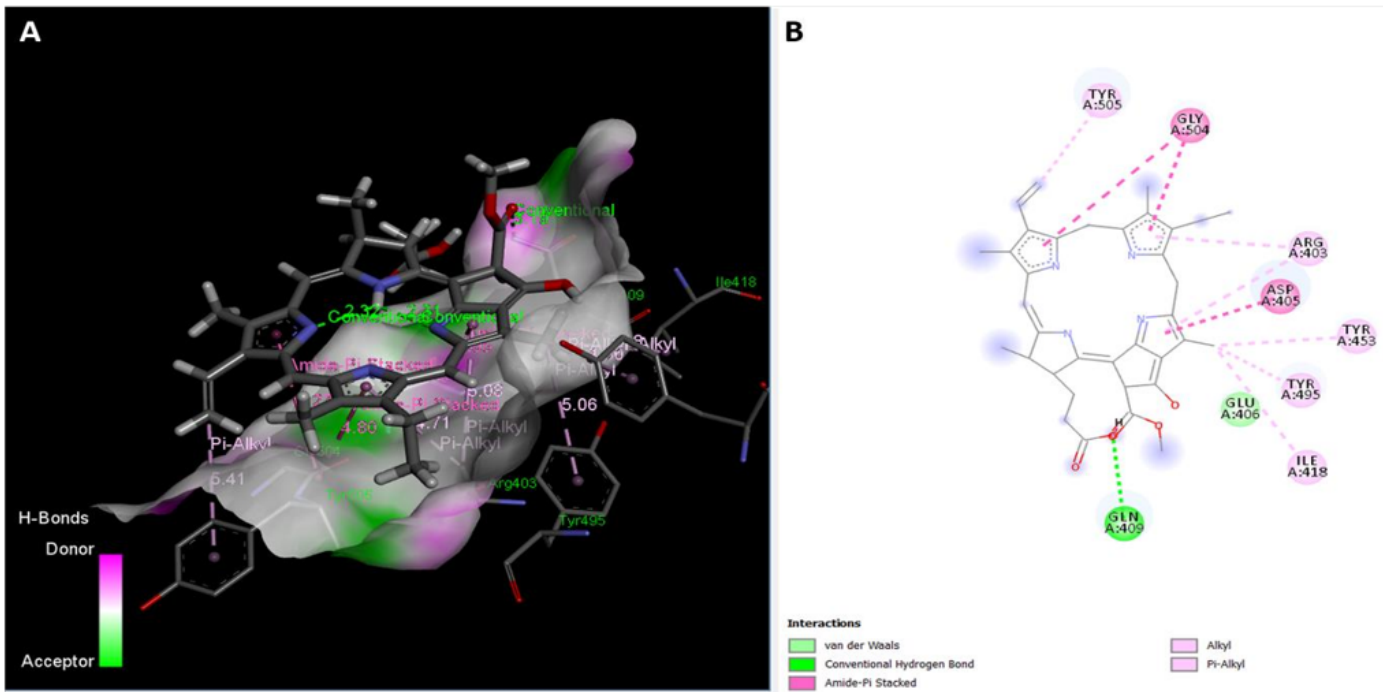


Figure 11

Three and two-dimensional interaction of pheophorbide A ligand with Spike protein RBD. A. Display of the receptor surfaces with H-bond contacts. B. 2D structure shows the ligand surrounded by active site residues, bond types, and distances.

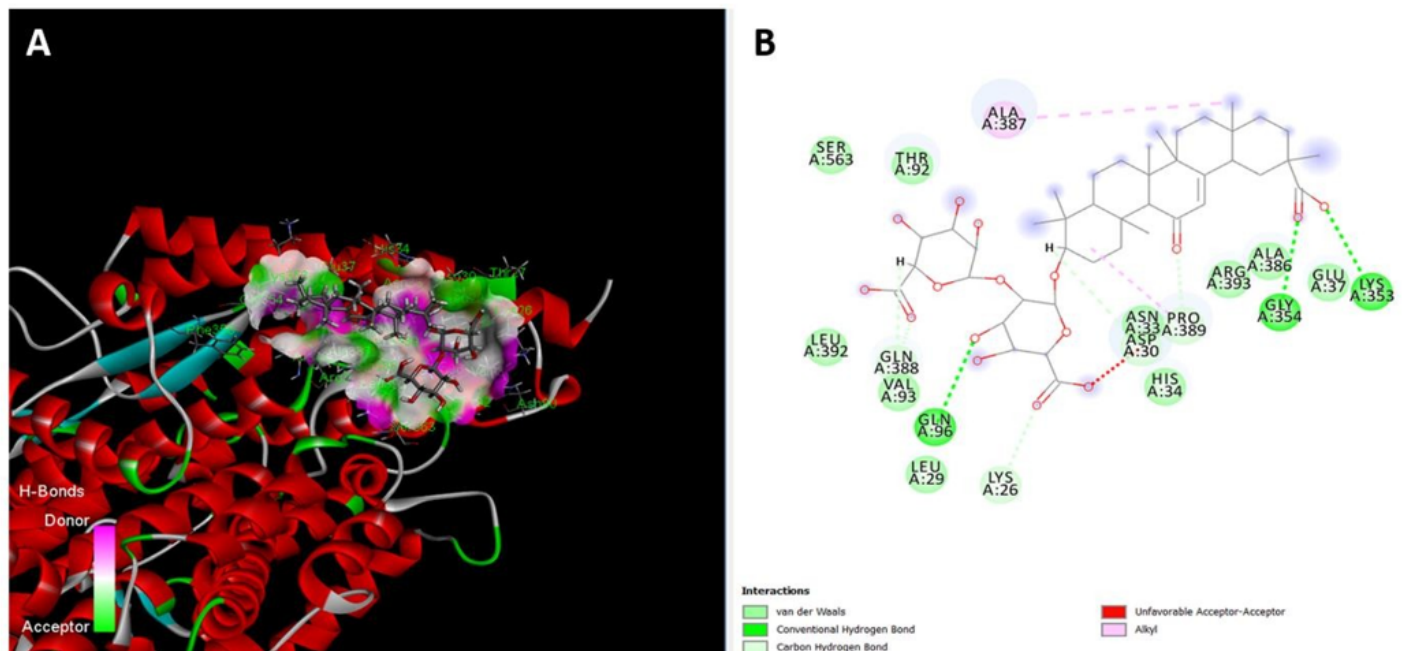


Figure 12

Three and two-dimensional interaction of glycyrrhizin ligand with ACE2. A. Display of the receptor surface with H bonds surrounding ligand-binding site. B. 2D structure shows the ligand surrounded by active site residues, bond types, and distances.

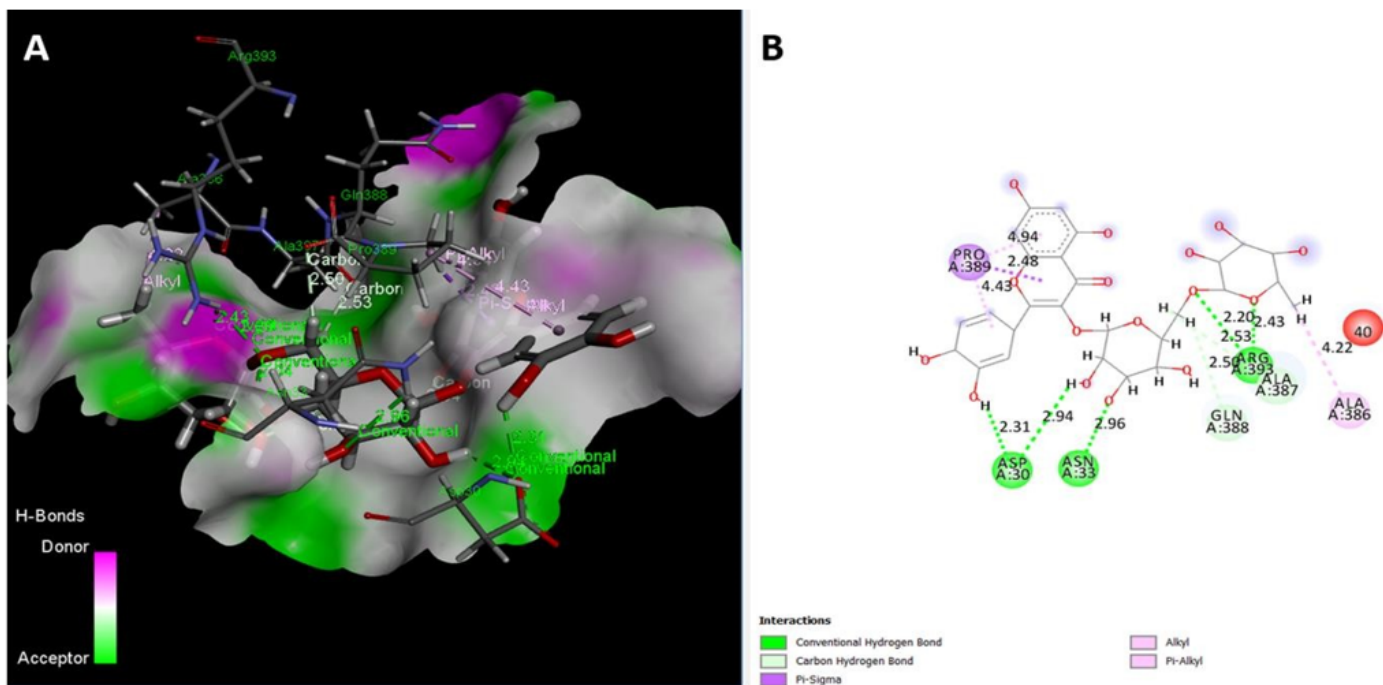


Figure 13

Three and two-dimensional interaction of rutin ligand with ACE2. A. Display of the receptor surface with H-bond contacts and ligand. B. 2D structure shows the ligand surrounded by active site residues, bond types, and distances.

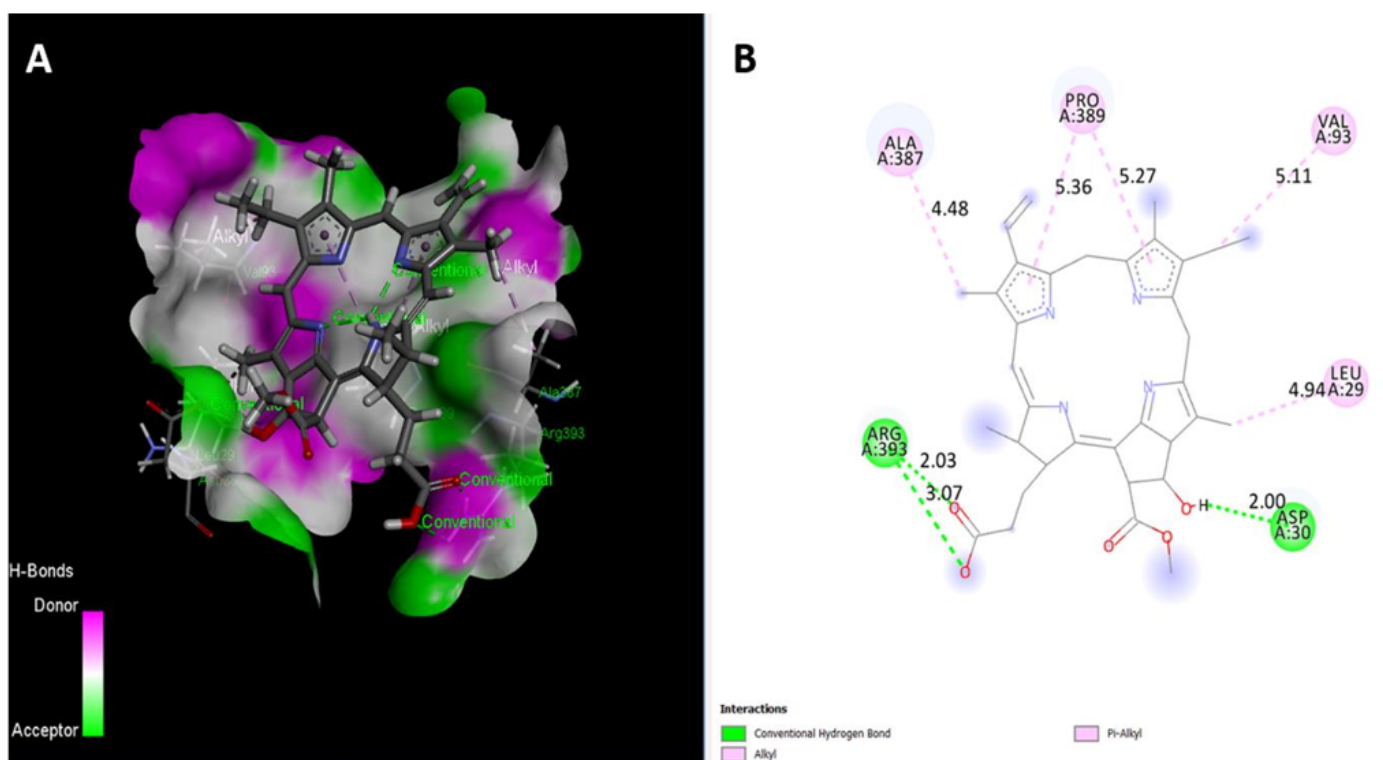


Figure 14

Three and two-dimensional interaction of pheophorbide A ligand with ACE2. A. Display of the receptor surfaces with H-bond contacts and ligand. B. 2D structure shows the ligand surrounded by active site residues, bond types, and distances.